EFDA–JET–CP(12)05/15

A. Huber, S. Brezinsek, Ph. Mertens, B. Schweer, G. Sergienko, A. Terra,
G. Arnoux, N. Balshaw, M. Clever, T. Edlingdon, S. Egner, J. Farthing, M. Hartl,
L. Horton, D. Kampf, J. Klammer, H.T. Lambertz, G.F. Matthews, C. Morlock,
A. Murari, M. Reindl, V. Riccardo, U. Samm, S. Sanders, M. Stamp,
J. Williams, K.D. Zastrow, C. Zauner and JET EFDA contributors

A new Radiation-Hard Endoscope for Divertor Spectroscopy on JET

A new Radiation-Hard Endoscope for Divertor Spectroscopy on JET

A. Huber[1], S. Brezinsek[1], Ph. Mertens[1], B. Schweer[1], G. Sergienko[1], A. Terra[1], G. Arnoux[2], N. Balshaw[2], M. Clever[1], T. Edlingdon[2], S. Egner[3], J. Farthing[2], M. Hartl[3], L. Horton[4], D. Kampf[3], J. Klammer[5], H.T. Lambertz[1], G.F. Matthews[2], C. Morlock[4], A. Murari[4], M. Reindl[5], V. Riccardo[2], U. Samm[1], S. Sanders[2], M. Stamp[2], J. Williams[2], K.D. Zastrow[2], C. Zauner[5] and JET EFDA contributors*

JET-EFDA, Culham Science Centre, OX14 3DB, Abingdon, UK

[1]Institute of Energy and Climate Research – Plasma Physics,, Forschungszentrum Jülich, EURATOM Association, Trilateral Euregio Cluster, D-52425 Jülich, Germany
[2]EURATOM-CCFE Fusion Association, Culham Science Centre, OX14 3DB, Abingdon, OXON, UK
[3]Kayser-Threde GmbH, D-81379 Munich, Germany
[4]EFD-JET Close Support Unit, Culham Science Centre, Culham, OX14 3DB, UK
[5]KRP-Mechatec Engineering GbR, D-85748 Garching b. Muenchen, Germany
** See annex of F. Romanelli et al, "Overview of JET Results", (23rd IAEA Fusion Energy Conference, Daejon, Republic of Korea (2010)).*

Preprint of Paper to be submitted for publication in Proceedings of the 27th Symposium on Fusion Technology (SOFT), Liege, Belgium
24th September 2012 - 28th September 2012

ABSTRACT

In preparation for ITER, JET has been upgraded with a new ITER-like wall (ILW), whereby the main plasma-facing components, previously made of carbon, have been replaced by Be in the main chamber and W in the divertor. A new endoscope with optimised divertor view has been developed in order to survey and monitor the emission of specific impurities such as tungsten, beryllium and the possibly remaining carbon in the tungsten divertor of JET-ILW. It operates in the wavelength range from 390nm to 2500nm with high optical transmittance (≥30%) as well as high spatial resolution, that is ≤2mm at the object plane and ≤3mm over the whole depth of field (±0.7m). The endoscope is a prototype for testing an ITER relevant design concept based on reflective optics only. The endoscope has an optimised observation in the near ultraviolet and in the blue spectral region to ensure the detection of the W I-emission line at 400.8nm.

In parallel to the new optical design, a new type of ITER-like shutter system based on pneumatic techniques has been developed and integrated in the endoscope head. The new optical design includes options for an in situ calibration of the endoscope transmittance during the experimental campaign.

1. INTRODUCTION

After the successful completion of the 2010-2011 shutdown, JET resumed operation with completely new plasma facing components (PFCs) consisting of a tungsten (W) divertor and a beryllium (Be) inner wall [1]. These PFCs have been selected for the DT phase of ITER to minimize the retention of tritium [2]. On the other hand, the operation of JET with ILW should be used to develop and demonstrate ITER-compatible scenarios within the material limits. The identification of the source of impurities and the measurement of their radiation distribution in front of all plasma-facing components is of fundamental importance for the understanding of physical processes such as power exhaust, detachment, recombination and recycling as well as of the erosion and redeposition properties.

As part of the diagnostic enhancements, a new, endoscope with optimised divertor view has been developed for this study in order to survey and monitor the emission of specific impurities such as tungsten, beryllium and the possibly remaining carbon in the tungsten divertor of JET.

In May 2011, the endoscope was successfully installed on the torus. It has delivered from the very first JET pulse images of the emission of the selected transition lines.

2. OPTICAL DESIGN AND MECHANICAL LAYOUT

The endoscope is a prototype for testing an ITER relevant design concept based on reflective optics only. The designed endoscope, excluding the detection system, should be able to sustain high neutron fluxes up to 10^{16} n^0 cm^{-2} s^{-1} as expected during JET operation. The diagnostic is located in octant 1, in a lower limiter guide tube (horizontal port at 330mm below the equatorial plane). The mechanical layout concept of the endoscope system as well as a schematic view of the optical design is presented in Figure 1. The endoscope is formed by the in-vessel tube that holds the optical head with front

mirrors. The optical system has been designed with a field of view of 16 degrees, viewing the divertor in both poloidal and toroidal directions. It provides information over a substantial portion of the toroidal extension of JET, i.e. more than 1/8th - 2/8th of the divertor. This large observation area avoids misinterpretation of measured data due to possible toroidal inhomogeneities.

The optical system consists of two main components: the endoscope optical head and the external telescope optical assembly. The optical head with entrance aperture and first mirrors is located in-vessel, i.e. in the vacuum, whereas the external telescope optical assembly is located outside the vessel.

The number of surfaces in the endoscope internal head has been reduced to two mirrors aiming for the optimization of the endoscope optical transmission. For an improved reduction of the stray light inside the in-vessel tube, four baffle apertures have been inserted in the beam path.
The vacuum interface is based on the double vacuum windows that are standard solution on JET used for tritium safety.
In this design we use fused silica, limiting thus the spectral measuring range to 2500nm. An exchange of the windows to achieve sufficient transmittance in the far IR wavelength range (for example sapphire) is possible. All mirrors have been manufactured by single point diamond turning procedures. The quality of all mirrors (the surface form errors and surface micro roughness) has been measured interferometrically by the mirror manufacturer. The Root Mean Square (RMS) surface form error and the RMS of the surface roughness of the endoscope mirrors are below $\lambda/10$.

Plasma particles influence the surface of the first mirror by erosion and deposition. Additionally, glow discharges used during the JET wall conditioning can significantly damage the surface of the in-vessel mirrors. Beryllium evaporation would lead to formation of layers on the mirror surface too, which degrades the reflection coefficient significantly.

The entrance aperture of the KL11 endoscope is equipped with a mechanical shutter implemented inside the JET vessel and operated in vacuum to minimise the degradation of the first mirror. Therefore, the shutter will be opened only before discharges in which measurements are performed. The time response for shutter movement between open and close positions (and vice versa) is about 30s.

The shutter system is operated pneumatically in a closed pressure circuit filled with neon to allow reliable function at all conditions at JET. In case of a leakage the amount of released neon does not jeopardise the JET vacuum and the shutter moves to an open position per default to guarantee continuation of the measurements. The rear side of the shutter is polished and used as a mirror to perform in situ transmission measurements in closed position.

The mechanical layout of the shutter system is shown in figure 2. The pneumatic piston carrying the shutter is mounted inside the endoscope head (see also Fig.3). A tube inserted inside the endoscope connects the pressure volume Vol-1 with a larger volume Vol-2 outside the vessel. Vol-2 has the maximal value when the shutter is open and the neon gas pressure is about 0.2bar. To close the shutter, the motor driven piston controlling Vol-2 is activated. Insertion of the piston reduces the volume Vol-2 and the pressure increases up to a factor of 20 to about 4.0 bar (displayed on the

pressure gauge). At this pressure, the piston at Vol-1 moves forward by 18 mm and the shutter is closed. For re-opening, the movement of the piston in Vol-2 is inverted. Detailed description of the shutter function can be found in [3] A Finite element method (FEM) multi-physics calculation was performed including the thermal and mechanical loads, to ensure that the endoscope shows no structural failure and that its performance is not affected. It revealed a thermal expansion of about 5 mm of the front head in the axial direction while it also permitted to find a resonance frequency of about 30 Hz, higher than the imposed lower limit of 14 Hz. On a more global point of view, the reserve factor (RF) of most components was kept higher than 5 even if it was a challenge to raise the RF of mirror M2 to about 1. Global static deformation of the endoscope was about 1.5mm.

Although concept and design were considered as partially validated by the global multi-physics analysis, certification and validation tests were nevertheless performed. The most critical one has been without doubt the vibration test, which searched for the low resonance frequency between 0 and 50 Hz at 7g in vertical direction and found it (for most directions and cases) around 20 Hz, a successful achievement beyond the 14 Hz specification. The endoscope also withstood the thermal baking test which brought it to thermal conditions comparable to operation (absolute values and gradients). The endoscope showed high stability of the line of sight during this test. This stability in measurement despite environmental loading was the main validation step.

More detailed information about thermo-mechanical and FEM analysis as well the detailed description of the thermal backing and vibration tests can be found in [4,5].

2.1. ENDOSCOPE HEAD

The endoscope optical head collects light and transfers an image of the FOV over a distance of approx. 2 m from the in-vessel optical aperture through the vacuum windows to outside the torus. There is an intermediate image plane, approximately at the interface between the endoscope head structure and the in-vessel tube, where a field stop has been positioned to block stray light. Figure 3 shows a schematic and mechanical view of the endoscope head optical design from the entrance aperture to the field stop position. The optics consists of a plane mirror M1 and a concave aspherical mirror M2. The entrance aperture stop is circular with a diameter of 8mm. The mirrors in the endoscope head are off axis and made of Al 6061 with an optical surface manufactured by single point diamond turning. The surface was left uncoated to mitigate a possible risk of degradation of the mirror coating in the in-vessel environment.

The entrance aperture has been fixed to the optical head in order to serve as a stable aperture stop. The entrance aperture is chosen small to prevent a transmittance degradation with time due to impurity deposition and erosion by fast neutral particles as well as to fulfil the requirements for the depth of field.

2.2. EXTERNAL OPTICAL TELESCOPE

The external telescope images the FOV, via the intermediate image generated by the endoscope head

optics, onto the focal planes of the various camera systems. It consists of a four-mirror aspherical off axis arrangement (TM1 – TM4) and a beam splitter unit, the first optical element of which is a reflective 50/50 beam splitter (BS). Figure 4 (top) shows a schematic overview of the external telescope. All mirrors TM1 – TM4, including the beam splitter BS, have been coated with Ag and a SiO2 protection layer to enhance reflectivity especially in the VIS wavelength range.

The materials of the mirrors and the structure have been chosen from aluminium (AL6061), a thermally treated forged material, in order to achieve a homogeneous thermal behaviour. All mirrors are mounted "stress free" with a three point support allowing alignment within the structure.

All optical components of the external telescope assembly as well as the detection system are located outside the vessel. The baseline design is a box-like structure with the four mirrors and 90° beam splitter (BS) integrated with fixations to the vacuum flange. The box is closed by means of a sheet of aluminium without structural support in order to reduce the stress induced on the optical elements.

3. PERFORMANCE

The spatial resolution of the designed endoscope shall be better than 3 mm at the object plane and the Depth of the Field of the endoscope should be DOF ≥ 1440 mm. For optical performance tests and for the verification of the FOV a mock-up of the JET divertor has been manufactured. The precise positioning of the endoscope and mock-up divertor has been done by the help of Photogrammetry. The MTF target has been located at distances of 5080mm, 4720mm, 4000mm, 3640mm, 3280mm and 2920mm. The images of the divertor mock-up with MTF target have been taken by every camera and the MTF has been calculated. Fig.5 shows the measured Modulation Transfer Function (MTF), for one camera. The camera was focused onto the object plane at a distance of 3640mm. The presented MTF represents the optical performance of the optical system of the endoscopes combined with the PIKE camera (see below); accordingly, the performance of the DES optical system alone is better than the presented one. As shown in Fig.5b, in the entire measured region between extremes, the MTFs show values larger than 50%. Thus the optical system fulfils completely the spatial resolution and DOF requirements.

The new optical design includes options for the in situ calibration of the endoscope transmittance during the experimental campaign, which allows the continuous tracing of possible transmittance degradation with time.

The in situ calibration unit contains the light source and the detector (spectrometer) –see description in [3]. The light is introduced backward in the endoscope optical system from the location of the camera and is be reflected from the rear side of the closed shutter (mirror surface) back to the detector. The first measurements (reference spectrum) were made with a combination of the in situ unit with a Ulbricht sphere. Later measurements should be compared with this reference spectrum. According to design requirements, the endoscope must cover the spectral range from 390 nm to 2500 nm with an optical transmittance T ≥30%. Figure 5c shows the endoscope transmittance recorded

directly after endoscope installation (reference transmittance) and the transmittance measured after 7 months of JET operation. The measured transmittance of the entire endoscope system for wavelengths $\lambda > 400$nm completely fulfils the requirements. They are still met after 7 months for wavelengths $\lambda > 500$nm For $\lambda < 500$nm we observe some degradation after 7 months of operation ($\Delta T \approx 40\%$ at 400 nm).

4. DETECTION AND FIRST RESULT

The endoscope is equipped with four digital CCD cameras: Allied Vision Technologies (AVT) Pike F-100B CCD camera, 1000×1000pixel, Pixel size: 7.4μm×7.4μm, FireWire data connection via optical fibres, max. 33 fps at full resolution and 16 bits data output. Each camera is combined with a filter wheel for narrow band interference (with a ≈1.5nm spectral bandwidth) and neutral density filters. Two of these cameras are equipped with micro-channel plate (MCP) image intensifiers (Proxitronic BV2562BZ, photocathode Ø25mm). All camera sensors are cooled to temperatures of about –10°C leading to a significant increase in the dynamical range of cameras. More description of the detection system can be found in [3].

Figure 6 shows the example of the Be II (527 nm)-emission profile taken during a density limit experiment with exposure times 30ms. The recorded images are inverted by a singular value decomposition method [6], to provide local emissivities. Figure 6b provides snapshot of the Be II-emission profile from L-mode density limit discharge ($B_T = 2.4$T, $I_p = 1.7$ MA, $P_{NBI} = 2.0$MW). During the recent JET experimental campaigns, the new endoscope clearly demonstrated the excellent resolution of the recorded images allowing high quality tomographic reconstructtion of the poloidal distribution of plasma species radiation.

SUMMARY

The KL11 endoscope was successfully installed in May 2011, more than 2 months before JET restart. The spatial resolution of the DES optical system delivers the expected optical performance in the operating wavelength range from 390nm to 2500nm: high optical transmittance (≥30%) as well as a high spatial resolution that is ≤ 2 mm at the object plane and ≤ 3 mm over the whole depth of field (±0.7m). The new optical design includes options for the in-situ calibration of the endoscope transmittance during the experimental campaign, which allows the continuous tracing of possible degradation with time. A new type of shutter system based on pneumatic techniques has been developed in view of ITER and integrated into the endoscope head.

ACKNOWLEDGEMENTS

This work, supported by the European Communities under the contract of Association between EURATOM and FZJ, was carried out within the framework of the European Fusion Development Agreement (EFDA). The views and opinions expressed herein do not necessarily reflect those of the European Commission.

REFERENCES

[1]. G.F. Matthews et al., Physica Scripta **T145** (2011) 014001

[2]. J. Roth, et al., Plasma Physics and Controlled Fusion **50** (2008) 103001 (20pp)

[3]. A. Huber et al., Review of Scientific Instruments **83**, 10D511 (2012); http://dx.doi.org/10.1063/1.4731759

[4]. A. Terra et al., this proceeding

[5]. C. Zauner et al., this proceeding

[6]. A .Huber et al., Journal of Nuclear Materials **313-316** (2003) 925.

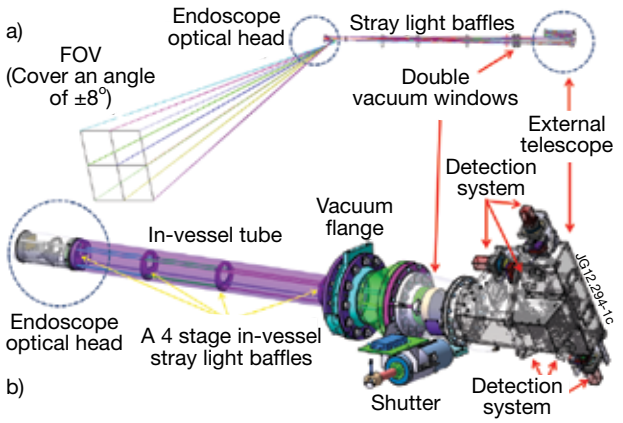

Figure 1: a) Optical design overview and b) mechanical construction of the endoscope system.

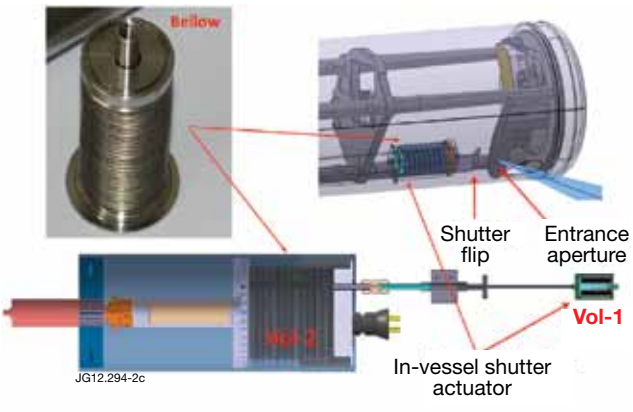

Figure 2: Mechanical layout of the shutter system.

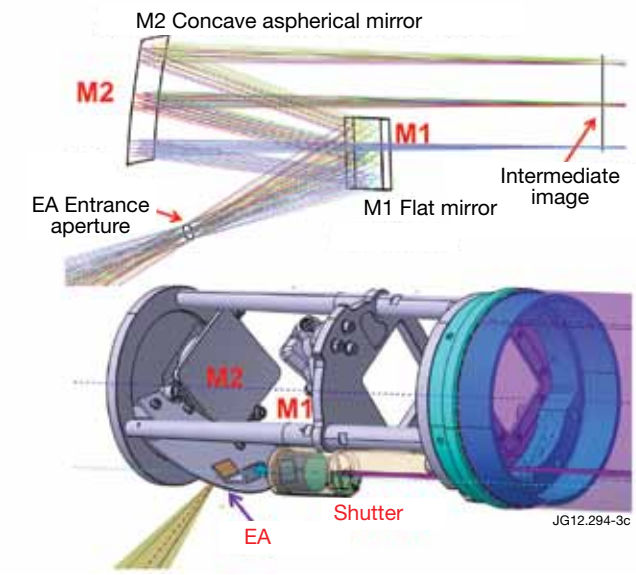

Figure 3:The endoscope optical head with in-vessel shutter actuator: a) optical design and b) the mechanical layout.

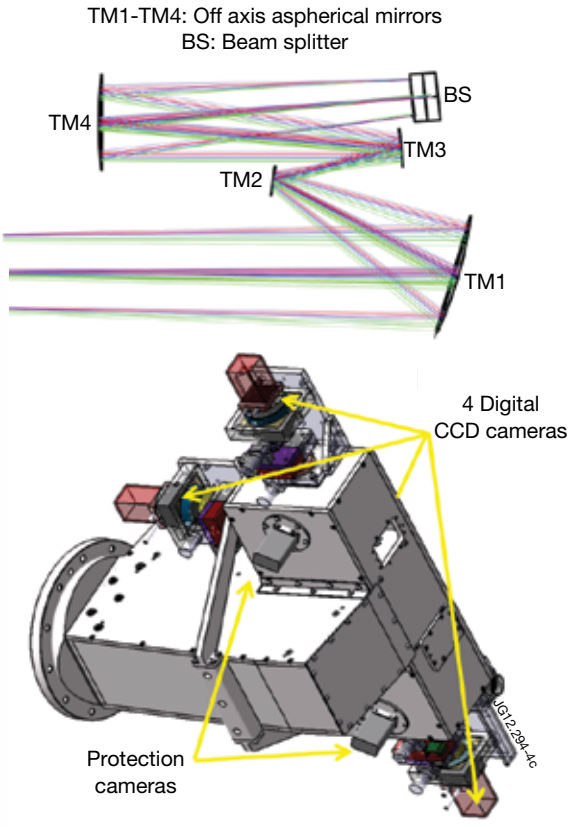

Figure 4: The arrangement of the external telescope: a) optical design and b) mechanical construct.

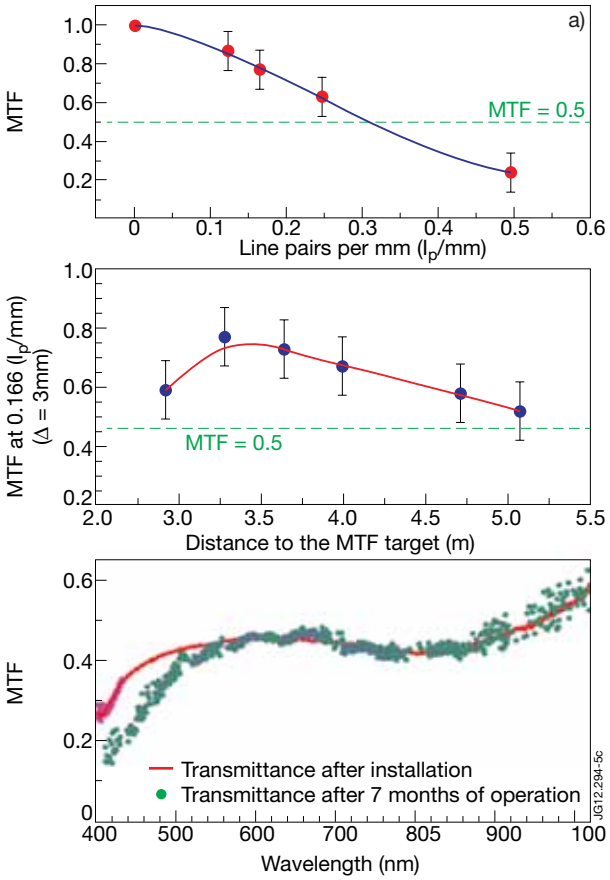

Figure 5: The measured Modulation Transfer Function (MTF): a) in the object plane and b) MTF at different distances from the entrance aperture at the spatialfrequency of 0.166 l/mm.The bottom figure shows the transmittance of the endoscope optical system.

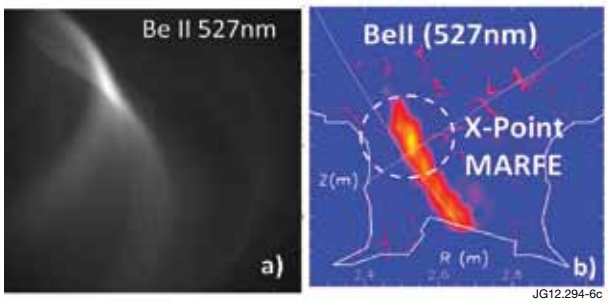

Figure 6: (a) Be II -emission image taken in the divertor region (b) tomographic reconstructions of BeII-emission.